Elevated Translocator Protein in Anterior Cingulate in Major Depression and a Role for Inflammation in Suicidal Thinking: A Positron Emission Tomography Study

Supplemental Information

Supplementary Methods and Materials

Past antidepressant use in MDD patients

Table S1. Details of previous antidepressants for each patient and number of months since last use, where applicable.

Patient	Previous antidepressants	Months without antidepressant
1	Citalopram	48
2	Citalopram	12
3	-	-
4	-	-
5	Sertraline, citalopram, fluoxetine, venlafaxine	12
6	-	-
7	Fluoxetine	60
8	-	-
9	Fluoxetine	8
10	Amitriptyline, mirtazapine	25
11	Reboxetine, sertraline, paroxetine	24
12	-	-
13	-	-
14	-	-

Methodological considerations

[^{11}C](*R*)-PK11195 was chosen in this study because, unlike [^{11}C]PBR-28, [^{18}F]DPA-714 and other second generation TSPO radioligands, its differences in binding affinity in humans due to the polymorphism rs6971 are negligible (1). This allowed us to include all eligible participants in this study regardless of binding affinity, including the approximately 10% of the population who are low affinity binders and therefore excluded from studies using second generation tracers (2).

We decided not to use an arterial input function due to the likelihood that the requirement for arterial cannulation would further limit recruitment of an already difficult to recruit clinical population (drug-free patients with major depression of at least moderate severity).

Therefore the quantification of regional [^{11}C](*R*)-PK11195 binding in the brain had to use a reference tissue input function. This brought in further requirements such as that the reference input is not affected by the disease, that its displaceable binding is insignificant relative to that in the target area and that of homogeneity of the non-displaceable binding across the brain. However, at the same time, results obtained from reference tissue analyses have proven to be more robust than those from plasma input function kinetic models in cases where it had been difficult to get reliable measurements of the fractions of unmetabolised tracer in plasma or of the plasma free fraction (3).

As TSPO expression is ubiquitous throughout the brain, there is no ideal reference region for PET studies assessing microglial activation with TSPO radioligands. An alternative is to use a pseudo-reference region, and our methodology used cerebellar grey matter (GM). Labelling of TSPO in post mortem human brain with [^{3}H]PK11195 found for the cerebellar cortex binding densities of 660 ± 85 fmol/mg protein in the granular cell layer, 191 ± 55 fmol/mg protein in the molecular cell layer and 41 ± 32 fmol/mg protein in white matter (4). For comparison, the highest binding densities were found in the dorsomedial thalamic nucleus (1912 ± 412 fmol/mg protein) and in inferior olivary nucleus of the medulla (1655 ± 355 fmol/mg protein). This amount of specific binding in the cerebellum causes an underestimation of the specific binding in the target regions of the brain, if a cerebellar input function is chosen for a reference tissue model.

Therefore, data driven approaches have been developed to extract the reference tissue kinetics from dynamic brain scans with [^{11}C](*R*)-PK11195 on the voxel level (5-7). These methods do not rely on an anatomically delineated region of interest for the definition of the reference region. Instead, they group voxels together based on their similarity between the voxel time-activity curves.

Supervised cluster analysis (SVC6)

We therefore also analysed our data using the alternative approach of supervised cluster reference input function (SVC6), a data-driven modelling method which segments voxels in the raw dynamic

data into six pre-defined tissue classes (normal grey and white matter, blood pool, muscle, skull and pathological tissue with high TSPO density) based on their time activity curves, then extracts as a reference region a cluster of GM voxels which exhibit kinetic behaviour closest to that of GM in a population of healthy controls.

Overall, BP_{ND} in our regions of interest derived from SVC6 were modestly underestimated and had higher variance (data not shown), with an associated reduced power to discriminate between-group differences, compared to BP_{ND} derived using the cerebellar GM input function. We therefore chose to present the latter data in our manuscript, in concurrence with papers which have concluded that the cerebellum is the preferred reference region over a supervised cluster region for [^{11}C](*R*)-PK11195 (8-10).

Validity of cerebellum as pseudo-reference region in MDD

The use of a pseudo-reference region such as the cerebellum is acceptable as long as there is no significant systematic difference in cerebellar uptake between healthy subjects and patients with MDD such as might occur if the cerebellum is involved in the disease process associated with MDD. To the best of our knowledge there are no published post mortem data on microglia in the cerebellum in MDD to support or refute the validity of cerebellar grey matter as a pseudo-reference region for TSPO imaging. However, using SVC6, cerebellum BP_{ND} values in our study were approximately mean-zero (in fact slightly negative) and not different ($p=0.77$) between healthy controls (-0.051 ± 0.057; $n=13$) and patients with MDD (-0.042 ± 0.095; $n=14$) (see Figure S1, below). We therefore found no evidence within our data to suggest that the study findings are confounded by a systematic difference in cerebellar TSPO binding between the control and patient groups.

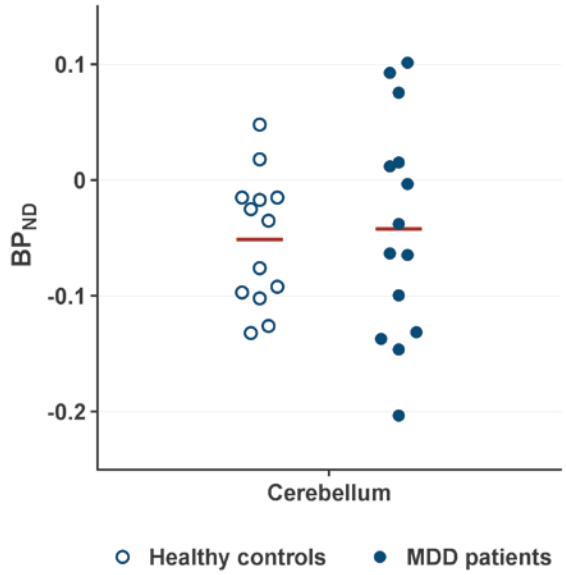

Figure S1. Cerebellum BP_{ND} values in healthy controls and MDD patients.

Effect of age on group comparison

Because there was no significant main effect of age on BP_{ND}, the main analysis did not include age as a covariate. However, for the sake of comparison we performed a secondary analysis with BP_{ND} in ACC, PFC and insula as the dependent variables, group (MDD or healthy controls) as the fixed independent variable, and introducing age as a covariate. This did not materially alter the statistical significances of the main effect of group ($F_{3, 22}$=5.40, p=0.006) or the between group differences: the elevation in the ACC remained of large effect size and statistically significant ($F_{1, 24}$=6.77, p=0.016; partial η^2=0.220; Cohen's d=0.95), and of small effect size and not statistically significant in PFC ($F_{1, 24}$=1.28, p=0.268; partial η^2=0.051; Cohen's d=0.38) and insula ($F_{1, 24}$=0.727, p=0.402; partial η^2=0.029; Cohen's d=0.29).

Voxel-based morphometry

A post-hoc voxel-based morphometry (VBM) analysis was carried out to examine possible differences in grey matter volume between MDD patients and controls. Image pre-processing was conducted using SPM12 (Statistical Parametric Mapping, Wellcome Department of Imaging Neuroscience, Institute of Neurology, London, UK) running in MATLAB R2015a (Mathworks,

Natick, Massachusetts). After realignment, the structural T1-weighted images were segmented into grey matter (GM), white matter (WM) and cerebrospinal fluid (CSF). A template was created and the deformations that best aligned the images were estimated using DARTEL (diffeomorphic registration). Then, spatially normalised and smoothed Jacobian scaled GM images were generated using the deformation images calculated in the previous step. For each volunteer GM tissue volumes were calculated. Finally, a GM analysis mask (thresholded at a belonging probability >0.2) was created in order to avoid instabilities that might occur in the analysis if the background is included. After pre-processing, a voxel-wise two-sample t-test was run in SPM12 comparing the smoothed, modulated, normalised, grey-matter images of our two groups. In this analysis we used the previously created GM analysis mask for explicit masking and the previously calculated tissue volumes for global calculation. Clusters of voxels were considered significant at a cluster-size threshold of pFWEc<0.05 and a height-threshold of p<0.001 (uncorrected).

Additional non-hypothesized regions

Table S2. TSPO availability ([^{11}C](*R*)-PK11195 BP_{ND}) for additional regions

Region	MDD patients (n=14)	Healthy controls (n=13)	% difference	Significance (p)
Parietal cortex	0.081 (0.077)	0.074 (0.024)	9%	0.76
Occipital cortex	0.058 (0.046)	0.048 (0.029)	20%	0.51
PCC	0.109 (0.064)	0.068 (0.024)	59%	0.04*
Hippocampus	-0.001 (0.082)	-0.027 (0.063)	-	0.37
Amygdala	0.017 (0.078)	-0.030 (0.053)	-	0.08
Thalamus	0.198 (0.080)	0.172 (0.071)	15%	0.38
Caudate	-0.084 (0.093)	-0.128 (0.104)	-	0.25
Putamen	0.103 (0.069)	0.088 (0.053)	17%	9.54
Brainstem	0.154 (0.051)	0.115 (0.066)	34%	0.10

Values presented as mean (SD). PCC: posterior cingulate cortex. P-values obtained from independent-samples t-tests. *significant at p<0.05, without correction for multiple comparisons.

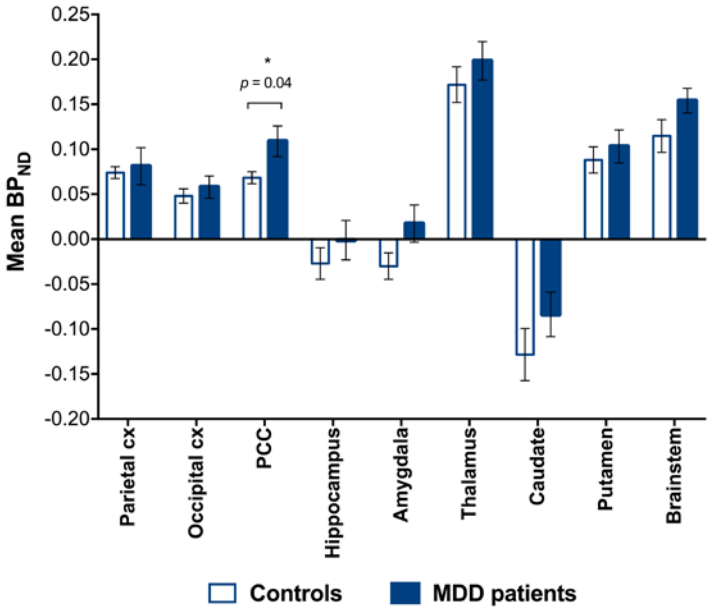

Figure S2. TSPO availability ([^{11}C](*R*)-PK11195 BP$_{ND}$) for additional regions

Supplementary References

1. Owen DR, Yeo AJ, Gunn RN, Song K, Wadsworth G, Lewis A, et al. (2012): An 18-kDa translocator protein (TSPO) polymorphism explains differences in binding affinity of the PET radioligand PBR28. *J Cereb Blood Flow Metab*. 32:1-5.
2. Kreisl WC, Fujita M, Fujimura Y, Kimura N, Jenko KJ, Kannan P, et al. (2010): Comparison of [(11)C]-(R)-PK 11195 and [(11)C]PBR28, two radioligands for translocator protein (18 kDa) in human and monkey: Implications for positron emission tomographic imaging of this inflammation biomarker. *Neuroimage*. 49:2924-2932.
3. Slifstein M, Laruelle M (2001): Models and methods for derivation of in vivo neuroreceptor parameters with PET and SPECT reversible radiotracers. *Nucl Med Biol*. 28:595-608.
4. Doble A, Malgouris C, Daniel M, Daniel N, Imbault F, Basbaum A, et al. (1987): Labelling of peripheral-type benzodiazepine binding sites in human brain with [3H]PK 11195: anatomical and subcellular distribution. *Brain Res Bull*. 18:49-61.
5. Banati RB, Newcombe J, Gunn RN, Cagnin A, Turkheimer F, Heppner F, et al. (2000): The peripheral benzodiazepine binding site in the brain in multiple sclerosis: quantitative in vivo imaging of microglia as a measure of disease activity. *Brain*. 123:2321-2337.
6. Turkheimer FE, Edison P, Pavese N, Roncaroli F, Anderson AN, Hammers A, et al. (2007): Reference and target region modeling of [11C]-(R)-PK11195 brain studies. *J Nucl Med*. 48:158-167.
7. Yaqub M, van Berckel BN, Schuitemaker A, Hinz R, Turkheimer FE, Tomasi G, et al. (2012): Optimization of supervised cluster analysis for extracting reference tissue input curves in (R)-[(11)C]PK11195 brain PET studies. *J Cereb Blood Flow Metab*. 32:1600-1608.
8. Holmes SE, Hinz R, Drake RJ, Gregory CJ, Conen S, Matthews JC, et al. (2016): In vivo imaging of brain microglial activity in antipsychotic-free and medicated schizophrenia: a [11C](R)-PK11195 positron emission tomography study. *Mol Psychiatry*. 21:1672-1679.
9. Kropholler MA, Boellaard R, van Berckel BN, Schuitemaker A, Kloet RW, Lubberink MJ, et al. (2007): Evaluation of reference regions for (R)-[(11)C]PK11195 studies in Alzheimer's disease and mild cognitive impairment. *J Cereb Blood Flow Metab*. 27:1965-1974.

10. Su Z, Herholz K, Gerhard A, Roncaroli F, Du Plessis D, Jackson A, et al. (2013): [11C]-(R)PK11195 tracer kinetics in the brain of glioma patients and a comparison of two referencing approaches. *Eur J Nucl Med Mol Imaging*. 40:1406-1419.